TRANSAT

Research and Innovation Action (RIA)

This project has received funding from the European Union's Horizon 2020 research and innovation programme under grant agreement No 754586.

Start date : 2017-09-01 Duration : 48 Months

Report on production of steel particles

Authors : Dr. Francois GENSDARMES (IRSN), Mickael Payet (CEA), Véronique Malard (CEA), Christian Grisolia (CEA)

TRANSAT - Contract Number: 754586
TRANSversal Actions for Tritium Project Officer: Angelgiorgio IORIZZO

Document title	Report on production of steel particles
Author(s)	Dr. Francois GENSDARMES, Mickael Payet (CEA), Véronique Malard (CEA), Christian Grisolia (CEA)
Number of pages	19
Document type	Deliverable
Work Package	WP03
Document number	D3.1
Issued by	IRSN
Date of completion	2019-02-08 15:40:36
Dissemination level	Public

Summary

The report details the steel particle production conditions and proposes a strategy for providing sufficient amount of steel powder for the in vitro and/or in vivo studies. In the first part, this work describes a method to produce and to characterise aerosols from cutting operations that represent decommissioning process within nuclear facility containing tritium. The result obtained makes it possible to calculate the airborne release fraction and aerosol size distribution in the case of 316 stainless steel piece cutting. In the second part, the very low production rate of steel particle from cutting leads to another strategy using a commercial powder. One powder is chosen and studied to act as surrogate powder. With an aerodynamic median diameter equal to 13.3 µm and a geometric standard deviation of 1.35, this powder is characterized by an inhalable fraction of particles equal to 72 %. The thoracic fraction is equal to 30 % whereas the respirable fraction is only 1%.

Approval

Date	By
2019-02-08 16:56:21	Mrs. Veronique MALARD (CEA)
2019-02-14 16:12:22	Mr. Christian GRISOLIA (CEA)

Table of contents

Index of Tables

Table of figures

This project has received funding from the Euratom research and training programme 2014-2018 under the grant agreement n°754586. The content in this report reflects only the views of the authors. The European Commission is not responsible for any use that may be made of the information it contains.

Abbreviations

ARF	Airborne Released Fraction
GF	Good Fellow
HEPA	High Efficiency Particulate Air
OPC	Optical Particle Counter

Summary

The report details the steel particle production conditions and proposes a strategy for providing sufficient amount of steel powder for the *in vitro* and/or *in vivo* studies.

In the first part, this work describes a method to produce and to characterise aerosols from cutting operations that represent decommissioning process within nuclear facility containing tritium. The result obtained makes it possible to calculate the airborne release fraction and aerosol size distribution in the case of 316 stainless steel piece cutting.

In the second part, the very low production rate of steel particle from cutting leads to another strategy using a commercial powder. One powder is chosen and studied to act as surrogate powder. With an aerodynamic median diameter equal to 13.3 µm and a geometric standard deviation of 1.35, this powder is characterized by an inhalable fraction of particles equal to 72 %. The thoracic fraction is equal to 30 % whereas the respirable fraction is only 1%.

1 Objectives

The first step in the objectives defined in the WP3 is the production of particles that represent decommissioning process within nuclear facility containing tritium. This task is divided in the following points: (i) Identification of the relevant steel and cement particles generated during decommissioning process in both fusion and fission. (ii) Production of such particles in sufficient amount for eco and toxicology studies. (iii) Characterization of these particles in term of their physical and chemical stability. (iv) Tritium loading of these particles.

This report deals only with the production of steel particles representing those obtained in decommissioning process except the tritium content. The cement particle production will be presented in the deliverable D3.2. The tritium loading is currently under study for steel particles, the results will be detailed in the deliverable D3.3 with those concerning cement.

The main source of steel particles containing tritium from decommissioning process is the cutting of pipe or structure component made of steel. In order to limit the tritium release, the cutting tool for steel would produce limited heat. Consequently, reciprocating saws are used for less thickness component (pipe or plate).

Considering the European standard EN 481, the particles of interest are below 100 µm in aerodynamic diameter. Discussions in WP3 Transat meeting lead to a maximum value of approximately 10 µm in aerodynamic diameter and a calculation of inhalable, throracic and respirable (alveolar) fractions taking into account precise particle size distribution.

The sufficient amount of particles means enough to manage radiotoxicology and ecotoxicology. Few grams were expected at the end of the 20-03-2018 meeting.

2 Cut particle production

2.1 The experimental set-up

2.1.1 Set-up description

The experimental set-up is in three parts: (i) the glove box that permits to confine aerosol and produced particles, (ii) the particle production device and (iii) the measurement system that allows the characterisation of the emitted particles.

The glove box, made of Plexiglas, has a volume around 250 L empty (Figure 1). HEPA filter is used on the air inlet to avoid background due to atmospheric aerosol. A pump coupled with a valve and a rotameter permits to control the air flow rate and the renewal of air in the glove box. The initial extraction flow rate is set at 183 ± 5 L/min. A membrane filter (FSLW type, Ø 47 mm) is installed at the air extraction of the glove box allowing the particles collection. The particles are produced during the stainless tube cutting maintained by a vice and using a reciprocating saw. An isoaxial sampling nozzle is set near the airflow extraction of the glove box in order to sample and measure the aerosol with an optical particle counter, *Grimm 1.109* (OPC). This instrument measures the size resolved number concentration in the size range of 0.25 to 30 µm (using 31 measuring channel).

- edge made of tungsten carbide, “S 1130 RIFF Basic for Cast Iron from Bosch

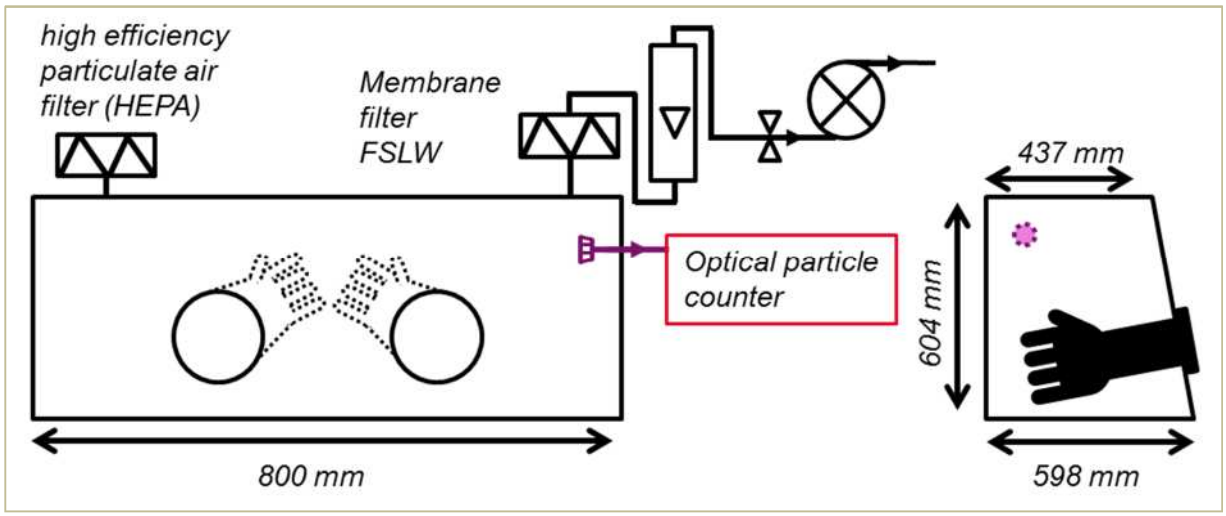

Figure 1: Scheme of the particle production set-up.

Two types of saw were used:

- *Bosch PSA7100E* (700 W) with a stroke rate reaching 2 700 strokes per minute
- *Makita XRJ06PT* (2×18 V) with variable 2-speed brushless motor delivering 0-2 300 (Low) and 0-3 000 (High) strokes per minute (Figure 2).

For the cutting, the usual edges are bimetal edges from the suppliers. However, this type of edge[1] are non-convenient for stainless steels, which are too hard. Therefore, a more resistant type of edge (*S1130 RIFF* from *Bosch*) was used for the following results. This edge is made of carbide.

Figure 2: Pictures of a) the *Makita XRJ06PT* saw and b) the *S1130 RIFF* edge made of carbide used for the cutting of stainless steel pipes.

2.1.2 Device qualification

For each campaign, the glove box is opened to place the cutting equipment (saw, tube and vice) then it is closed. Consequently, the starting aerosol in the glove box corresponds to the atmospheric aerosol in the laboratory air. The Figure 3 represents the evolution of the total number concentration (particle range size from 0.25 to 30 µm). From 0 s to 700 s, the particle concentration corresponding to the atmospheric aerosol is stable. Then, it decreases exponentially as soon as the pump is running (from 744 s) and HEPA filtered air is entering the glove box. Finally, the concentration plateau is below 10^3 particles/L. This stage points out an input term of particles in the glove box probably due to micro leaks and the depression in the box compared to the atmospheric air. As this final atmospheric particle concentration is considered negligible, the

[1] For this study, results seems similar whatever the edge but the life time of the special edge is more suitable for the experiments.

concentration evolution, in the glove box, can be described by the following relation (neglecting also the particle deposit in the glove box):

$$C_n = C_n^0 \times e^{-\frac{t}{\tau}} \ , \qquad (1)$$

where C_n^0 represents the particle concentration at the initial state, $\tau = V/Q$ is the time constant of air purification, Q is the filtered air flowrate, V is the effective volume of the glove box and t is the time.

The experimental time constant obtained by fitting the equation 1 on the experimental data is 72 ± 4 s. Consequently, each run of particle production was carried out after a purification time of 10 min (> 5×τ) to guaranty the renewal of air by filtered air in the glove box. The theoretical time constant τ_{theo} is equal to 81 s. This is a higher value than the experimental one because the effective volume should take into account the volume of all the elements inside the glove box (gloves, saw, vice…). Thus, the effective volume assessed by the experimental time constant τ is 219 L.

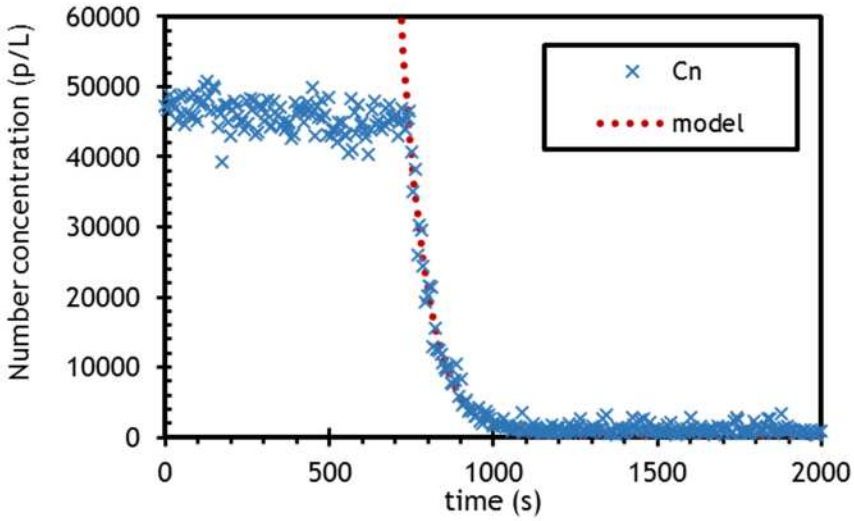

Figure 3: Evolution of the number concentration (p/L) in the glove box from atmospheric air to HEPA filtered air. The decreased model is superimposed to experimental data.

2.2 Background aerosol production due to the saw

2.2.1 Saw with carbon brushes

The first experiments were carried out with the Bosch saw. It works with an electric motor using graphite brushes which conduct the current from the static part to the moving part of a rotating shaft. These brushes are known to be altered during the working and consequently produce aerosol with graphite particles. The Figure 4 represents the total concentration of the aerosol in the glove box. The first plateau, from 0 s to 270 s, corresponds to the atmospheric aerosol. At 270 s, the decrease is due to the air renewal by HEPA filtered air using the pump. The second plateau between 500 s and 880 s is the particle background due to small leaks of the glove box operated in depression compared to atmosphere; the value is below 10^3 particles/L. At 880 s, the saw is working without cutting during 5 minutes (from 880 s to 1160 s) but not continuously; the saw is set on for 18 s then set off for 6 s. This sequence induces an increase in aerosol concentration only due to the particle emitted by the saw. Besides, after 900 s, the concentration exceeds 2×10^5 particles/L.

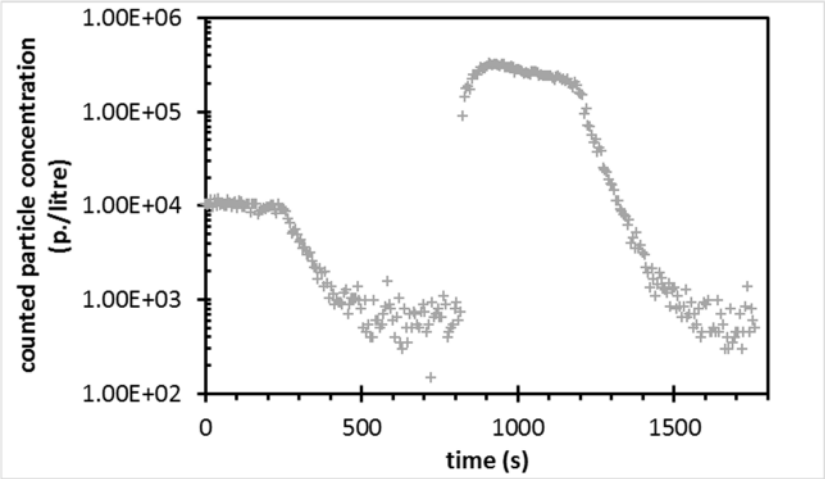

Figure 4: Evolution of the number concentration in the glove box during the saw working without cutting (saw with carbon brush).

It can be assume that the particles come from the friction of the carbon brushes. Consequently, in the following experiments, a brushless saw was used in order to avoid carbon particle pollution.

2.2.2 Brushless saw

The background noise is controlled when the saw is off and when the saw is running without cutting. For the latter, runs of 15 minutes were performed: 20 s of saw-working alternates with 10 s of shutdown. The Figure 5 represents the aerosol concentration in the glove box due to the saw running without cutting. A steady state is reached with a concentration approximately of 3×10^4 particles/L. This level is one order of magnitude lower than the one observed using a saw with carbon brushes. After the saw shutdown, another exponential decrease is observed with a purification time constant of 70 ± 4 s. After this purification phase, the background aerosol plateau reaches a background concentration below 10^3 particles/L.

We can suppose that this residual particle background comes from the friction of mechanical piece of the saw, probably the edge. It is sure that the pollution is due to the operation of the saw and it cannot be avoided. Besides, it can be noticed that the background is reduced significantly from the saw with carbon brushes to the brushless saw.

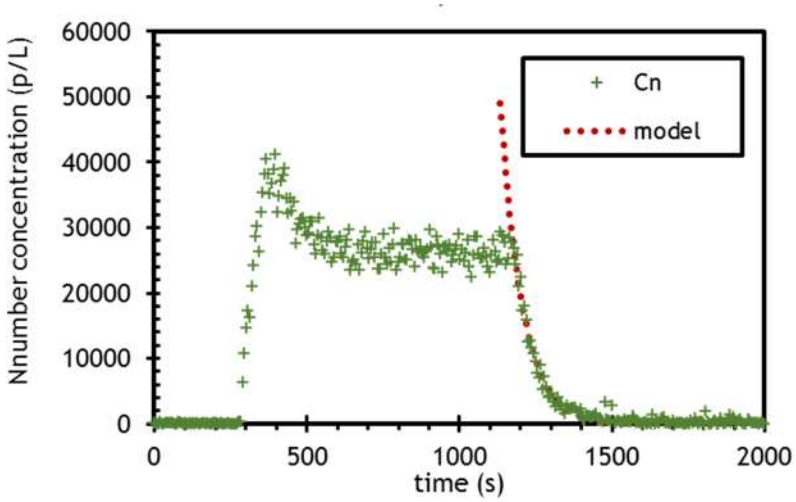

Figure 5: Evolution of the number concentration in the glove box during the saw working without cutting (brushless saw). The concentration-decreased model is superimposed to experimental data.

2.3 Steel particle production by saw cutting

2.3.1 Material

The TRANSAT WP3 focused on stainless steel from nuclear facilities, *i.e.* the 300 type, especially 304 and 316 (Table 1). Stainless steel of type 304 was used for preliminary tests (not shown here but presented during meetings). Indeed, the composition and the microstructure of both alloys are similar. The results are in the same order of magnitude considering these two similar stainless steels. The letter "L" means **Low** content of carbon (in the type 304 and 316, the maximum carbon content is 0.08 wt %).

Table 1: Mass composition (wt %) of the 304L and 316L stainless steels

Type	Fe	Cr	Ni	Mo	Mn	C
304L	Bal.	18-20	8-12	-	< 2	< 0.03
316L	Bal.	16-18	10-14	2-3	< 2	< 0.03

Both 316L and 304L steels present a face-centered cubic lattice (called austenite) that can be modified to a tetragonal lattice (martensitic phase) under severe strains. This phase transformation can be observed using a magnet: the martensitic phase is magnetic whereas the austenite is non-magnetic. In our study, the produced powder by reciprocating saw cutting is clearly magnetic.

In the present work, tube of stainless steel type 316L is studied. Two kinds of tube were used (see Table 2)

Table 2: Characteristics of the samples.

sample	External diameter (mm)	Thickness (mm)	Length (mm)	Mass (g)
Tube 1	12.7	1.62	329	114.434
Tube 2	9.5	1.12	419	83.693

2.3.2 Particle production in the glove box

The Figure 6 presents the particle concentration during two phases: from 700 s to 2 400 s, the saw is running and cutting steel whereas from 3 200 s to 4 200 s, the saw is running without cutting. Between each phase, the level concentration plateaus at the background noise level after the purification time. The comparison with the saw working to the saw cutting shows number concentration levels in range from 3×10^3 particles/L to 8×10^4 particles/L. The steel cutting induces a significant increase of the particle concentration in the aerosol but this comparison needs to be detailed in order to characterise the steel particles. The mass concentration is calculated from number concentrations measured by OPC and from particle mean masses for each i channel diameter assuming spherical particles and density equal to 8000 kg/m^3.

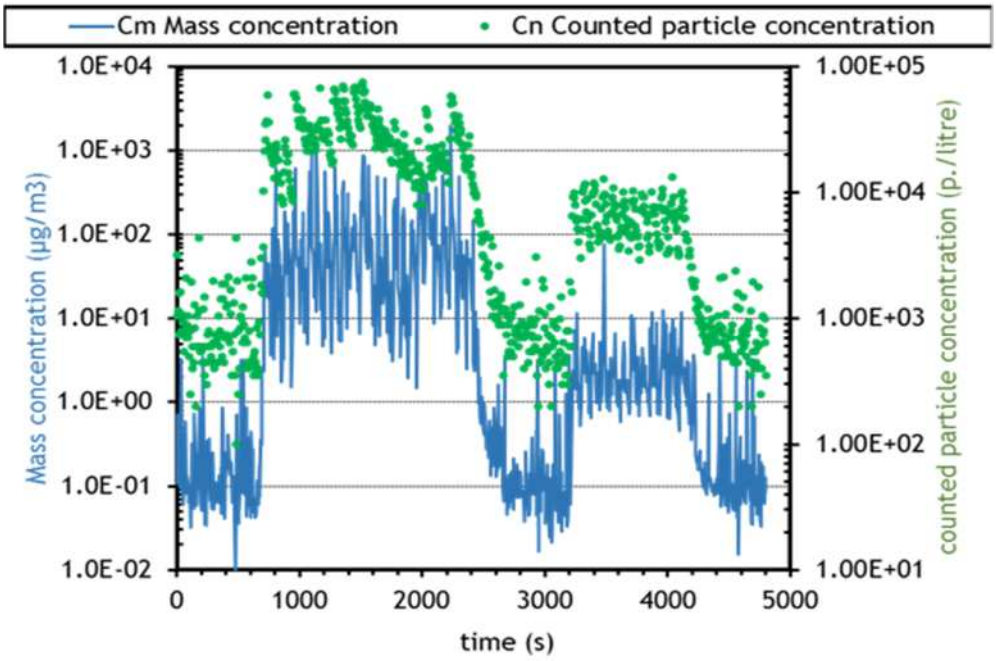

Figure 6: Evolution of the aerosol number concentration (green dots) and mass concentration (blue line) from background noise to steel cutting and to saw running without cutting.

2.3.3 Characterisation of the particles

To better identify the particles produced during the steel cutting, the comparison of the geometric mean diameter from the mass size distribution, d_g, permits to distinguish the different situations (cutting, background due to the glove box leaks or background due to the saw itself). This diameter d_g is calculated from number concentrations C_{n_i} measured by OPC and from particle mean masses m_i for each i channel (1 to 31) assuming spherical particles.

$$d_g(t) = \left(\prod_{i=1}^{31} {d_i}^{C_{n_i}(t)\times m_i}\right)^{\frac{1}{\sum_{j=1}^{31} C_{n_j}(t)\times m_j}} \quad . \qquad (2)$$

The Figure 7-a presents the evolution of d_g with time during a steel cutting which can be compared with the background noise (baseline). The Figure 7-b presents the d_g evolution with time during the saw operation without cutting. For those figures, the first part, approximately from 0 s to 600 s, corresponds to the background aerosol after purification and before the saw operation. In these cases, d_g is 0.35 µm in average on the 0 s – 600 s period. When the saw is running without cutting, d_g increases to 0.82 µm (average between 800 s and 1 600 s). The geometric mean diameter d_g increases significantly to 4.1 µm in average when the saw is cutting a steel piece. Consequently, particles produced can be clearly identified by their size to distinguish their origin, emitted by the saw operation or by the steel cutting: the particles presenting a diameter superior to 1 µm are mainly the expected ones from 316L steel. Note that these diameters correspond to optical equivalent diameters has measured by the *Grimm 1.109 OPC*.

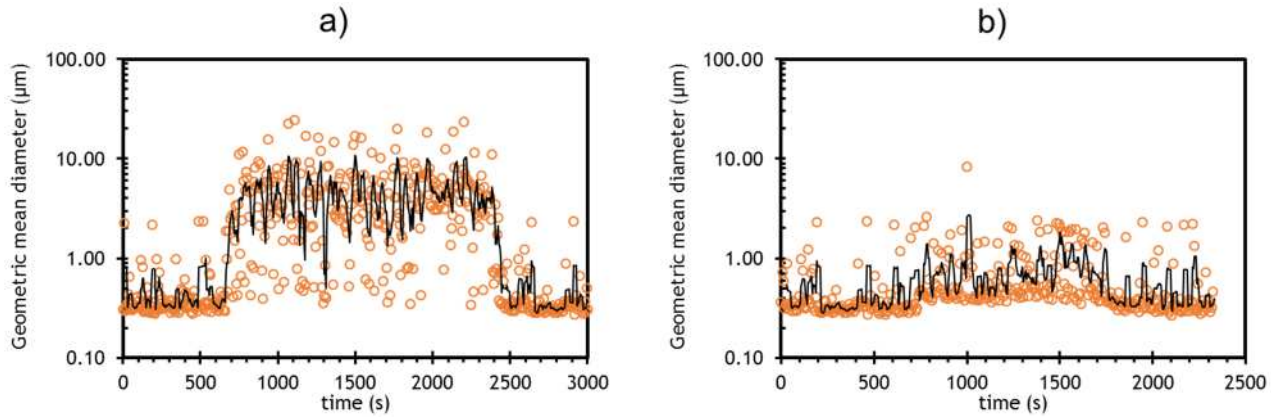

Figure 7: Mass geometric mean diameter a) from aerosol produced by stainless steel cutting, b) from aerosol emitted during saw running without cutting. Circle: measure on 6 s. Black line: moving average on 6 values.

Some particles in the range of 2 to 5 µm were observed using a scanning electron microscope (Figure 8). EDS analyses were performed to select the 316L steel particles from other particles as Au-Pd particles used to metallise the sample or other particles (see Annexes). No characteristic shape is observed but almost irregular shape particles like micro cutting ships.

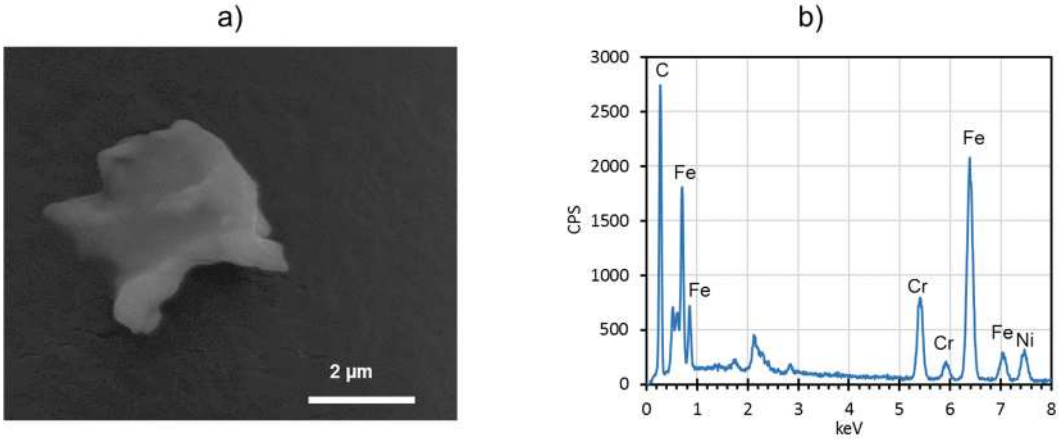

Figure 8: SEM observation at 20 kV of a particle collected on a filter: a) secondary electron image of a steel particle, b) EDS spectrum of the steel particle.

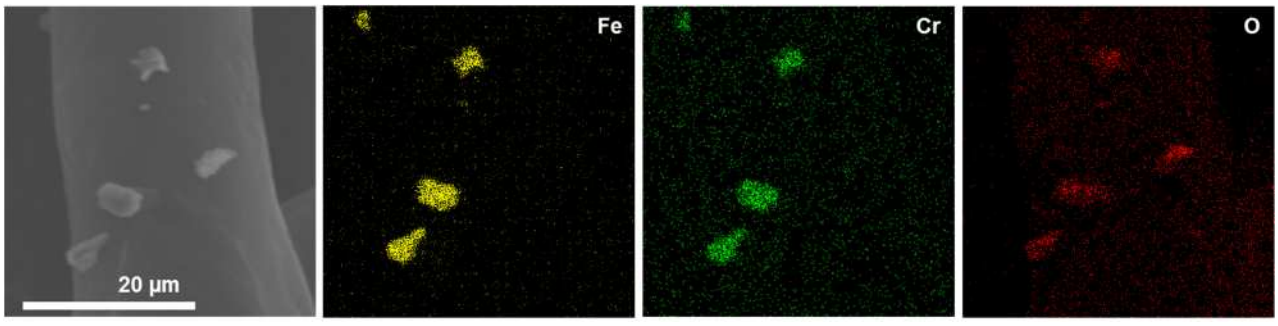

Figure 9: SEM map at 20 kV of collected particles on a fibre of the filter.

2.3.4 Emission rate of the steel aerosol

To analyse the results taking into account the steel particle losses by sedimentation in the glove box, we use an analytical model considering the aerosol concentration evolution (Gensdarmes, 2003). This model assumes a homogeneous concentration in the glove box at every time step. The applied parameters concern purification time constant, the sampling time, the size distribution of the aerosol and geometrical parameters of the glove box (volume and deposit surface). Based on equation 1 and the settling velocity of the steel particles, this model allows the calculation of a particle transfer efficiency coefficient I. Indeed, the whole aerosol mass m_d dispersed during a cutting is linked to the aerosol mass m_c at the exhaust and collected by the filter:

$$m_c = I \times m_d \quad . \tag{3}$$

Using a particle diameter of 4 µm, a particle density for steel equal to 8 000 kg/m^3, an effective glove box volume of 219 L (see 2.1.2), a sampling flow of 185 L/min and a deposition area of 0.48 m^2 (corresponding to glove box floor), the transfer coefficient I is equal to 0.62.

Thus $1 - I = 0.38$ represents the loss fraction by settling in the glove box during the collection. In the following, I coefficient is used for the assessment of the particle emission rate from mass of aerosol collected.

The set-up measures in two ways the emitted particles, the OPC and the filter. The OPC permits to estimate the emission rate r_{OPC} from data obtained in the range size above 1 µm. The equation is:

$$r_{OPC} = \frac{Q}{I} \times \overline{C_m} = \frac{Q}{I} \times \frac{1}{p} \sum_{k=1}^{p} \sum_{j=12}^{31} C_{n_j}(k) \times m_j \quad , \tag{4}$$

$\overline{C_m}$ is the average of the mass concentration during a cutting, p is the number of measurement during the cutting. The channel $j=12$ corresponds to the first size bin above 1 µm.

The second method is applied at the end of a run: the filter is weighted. In that case, the emission rate r_{filter} is calculated from the accumulated mass Δm_{filter} and the cutting time Δt_c:

$$r_{filter} = \frac{1}{I} \times \frac{\Delta m_{filter}}{\Delta t_c} \quad . \tag{5}$$

The Table 3 resumes the obtained data and results from both methods. The results are in the same range but emission rates from OPC data are below the value obtained by accumulated mass. This deviation is probably due to the hypotheses used for mass concentration calculations from number size distribution measured by the OPC (spherical particles for example, particle refractive index).

Consequently, the aerosol emission expressed as particle airborne released fraction ARF is calculated from filter mass corrected by transfer coefficient I and divided by the mass loss by the steel cut piece Δm. The uncertainty on the mass of aerosol collected with this kind of filter, determined by method from the standard ISO 15767, leads to relative uncertainty below 10 %.

Table 3: Mass loss by the steel cut piece, accumulated mass on the filter, rate emission, airborne release fraction for stainless steel 316L tubes.

Sample	Δm (mg)	Δm_{filter} (mg)	r_{OPC} (µg/min)	r_{filter} (µg/min)	ARF
tube 316-1	7793	1.6	48	69	3.3×10^{-4}
tube 316-2	11414	2.0	39	73	2.8×10^{-4}

The obtained values are consistent with those obtained by Bernard *et al.* (1998). Their study was performed in real scale with a volume of 32 m^3 and an airflow of 5 000 L/min. The time constant is 384 s. The studied materials are flat plates of mild steel or 304L stainless steel with a thickness range between 5 to 50 mm. Finally, the aerosol ratio for stainless steel is increasing with the thickness of the plate from 1.2×10^{-4} (for 5 mm of thickness) to 6.7×10^{-4} (for 50 mm of thickness).

Newton *et al.* (1987) studied also aerosols from metal cutting techniques typically used in decommissioning nuclear facilities. They collected particles from cutting in a full scale enclosure with a volume approximately of 26 m^3 and an airflow of 8 500 L/min. In these conditions, the time constant is 184 s. In this work, the studied material is also 304L. The particle distribution from a reciprocating saw is described bimodal: particles below 0.7 µm of diameter and particles in the range of 2.5 to 4.3 µm of diameter. The author report also the weakest rate emission for the reciprocating and the band saws compared to other cutting tools.

In any case, a small volume as in our set-up is not sufficient to improve significantly the production yield. The particle emission rate is weak and only a couple of milligrams have been collected for several hours. This method will not provide few grams of steel particles in acceptable time.

3 Use of surrogate particles

The difficulty to produce and collect sufficient particles of stainless steel lead us to an alternative method: the characterisation of the particles produced by cutting in order to define the parameters for using surrogate particles. Consequently, 316L powder from Goodfellow (reference FF216030 from Goodfellow Cambridge Limited, Huntingdon, England) was supplied with a mean diameter around 3 µm (factory data). This powder will be named GF powder in the following.

In order to adjust the surrogate particles to the cut particles, the characterisation of the commercial powder was performed.

3.1 Characterisation of the commercial powder

The characterisations were carried out at the IRSN using a SEM type JSM-6010-LA from JEOL, an optical microscope type Malvern® *Morphologi G3* and an TSI® *Aerosizer* powder sizer.

The SEM observations (Figure 10) show that particles are spheroidal whatever their size. Images reveal particle sizes from 1 µm to 8 µm.

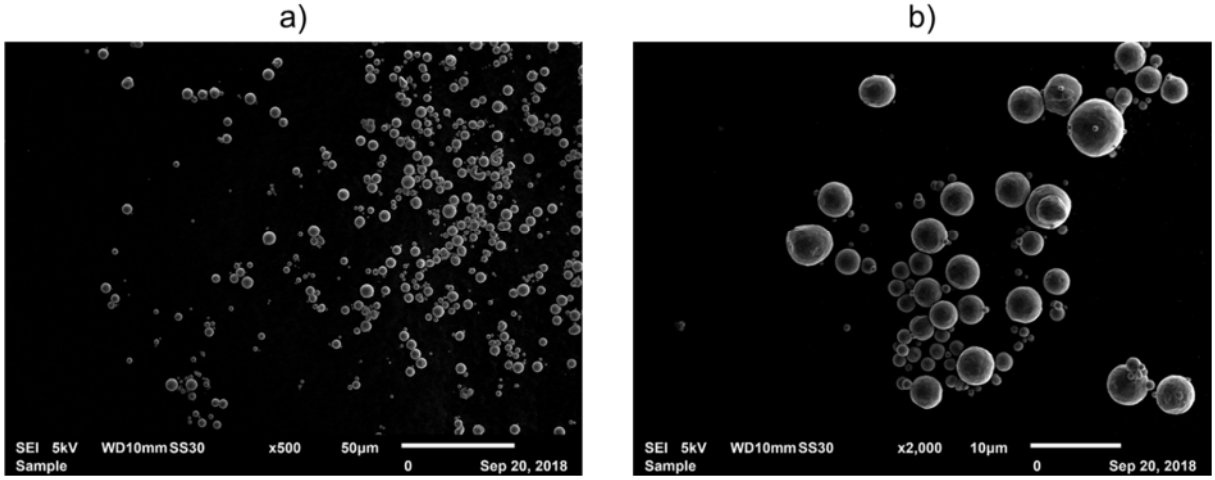

Figure 10: SEM observations (at 5 kV using secondary electrons) of steel particles from GF powder at two magnifications a) × 500, b) × 2 000.

Measurements performed using the optical microscope *Morphologi G3* and the *Aerosizer* are both expressed in terms of particle number and particle volume (i.e. mass). It should be notice that both instruments are based on particle number detection, the particle volume is calculated assuming spherical shape.

The results show large discrepancy between the number size distributions measured by the two instruments. The *Aerosizer* reveal that a large number fraction of the particles are below 1 µm. The optical microscope probably doesn't detect such fine particles due to optics configuration and image analysis configuration used for data processing.

The volume particle size distribution determined by the two instruments is also different. The size distribution measured with the *Aerosizer* exhibit a bimodal shape with particle above 10 µm. Such particles are not observed by the optical microscope. This result could be explained by a better powder dispersion process before particle size analysis with the optical microscope. Each instrument has its own powder disperser and no specific action could be done on that. Consequently we consider that the optical microscope give the reference mass distribution of the particles.

The mode measured by the *Morphologi G3* is 4.9 µm. As shown figure 11, the particle size distribution could be fitted by a lognormal function with a volume median diameter equal to 4.7 µm and a geometric standard deviation of 1.35. This lognormal function allows to calculate in a simple manner the different fractions of the aerosol regarding inhalation probability.

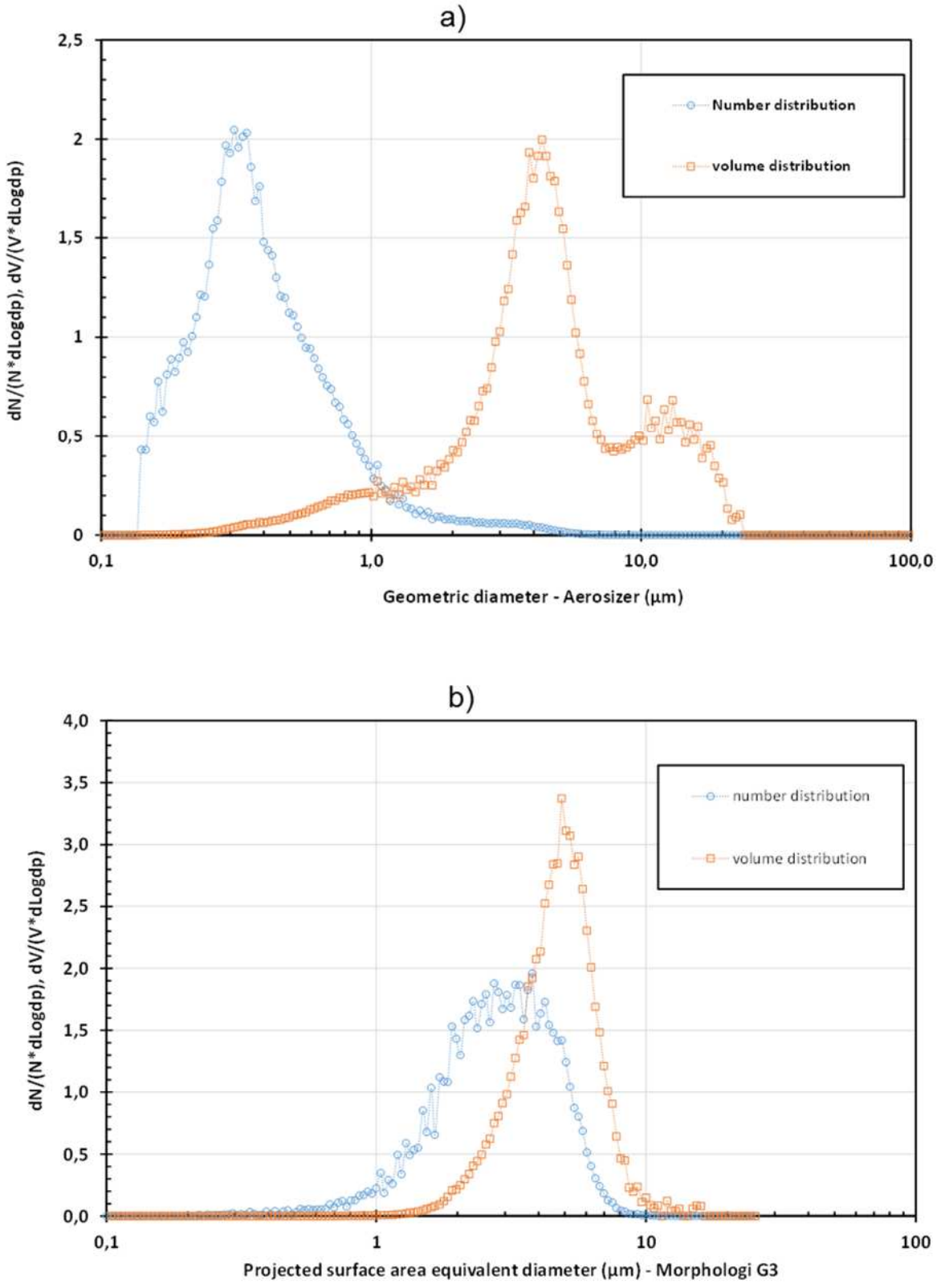

Figure 11: Number and volume distribution of the commercial powder measured using a) the Aerosizer and using b) the optical microscopy.

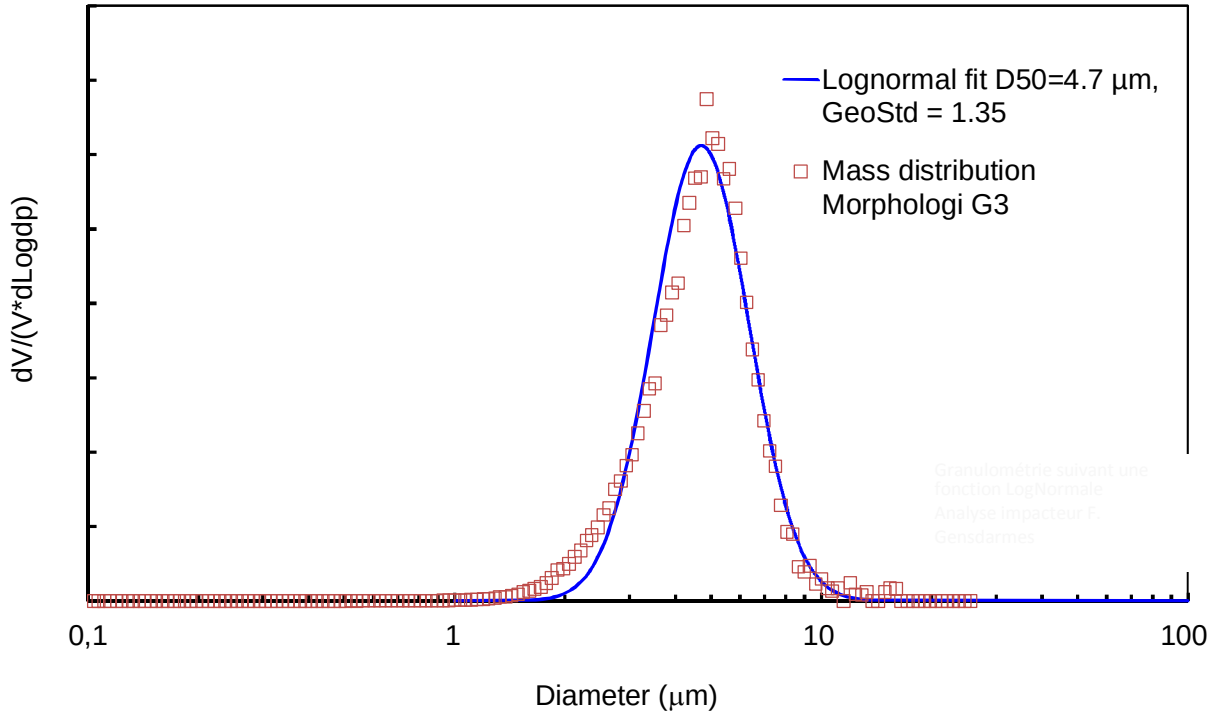

Figure 12: Volume size distribution measured by the Morphology and fitted with a lognormal function

Inhaled aerosols are fractionated during penetration into the airways. Penetration efficiency is a function of many physical and physiological parameters but in general it increases as particle size decreases. Only part of the total ambient aerosol is inhaled and only the finest particles reach the deep lung, i.e. alveolar region (Renoux, 1998).

On the basis of cutting into three anatomical regions of the respiratory tracks, is defined in occupational hygiene three fractions of an ambient aerosol in relation to potential health effects. These fractions are called Inhalable, Thoracic and Respirable (corresponding respectively in French to *Fraction Inhalable, Fraction Thoracique* and *Fraction Alvéolaire*).

It is in the context of collective prevention that these three fractions of an ambient aerosol have been defined and unanimously adopted in the form of a convention by the various organizations, namely the European Committee for Standardization, the International Organization for Standardization and the American Conference of Governmental Industrial Hygienists. These fractions are presented in Figure 13 as a function of the aerodynamic diameter of the particles. This virtual diameter is the relevant particle characteristic for micron size to assess particle behaviour (transport, deposition) regarding airflow. The aerodynamic diameter of a particle integrates its geometric diameter (equivalent volume or mass), its density and its shape; it is established, based on an equivalence of particle relaxation time, which characterises the time needed for the particle to adjust its velocity vector to a change in carrier fluid vector.

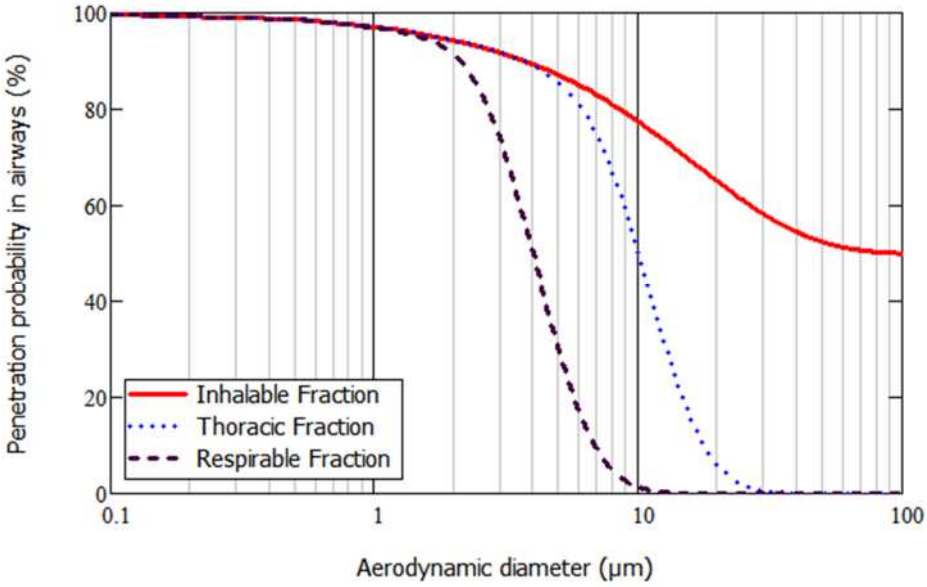

Figure 13: Conventional fractions of aerosol dealing with occupational exposure. (Baron, 2001 and Vincent, 1995)

The aerosol penetration in the lung is a function of aerodynamic diameter. The first step to assess the different conventional fractions is to calculate the median aerodynamic diameter of the aerosol from the size distribution measured by the *Morphologi G3*.

For irregular shape and non-porous particles, the aerodynamic diameter is linked to other particle characteristics by the relation:

$$\rho_0 \cdot d_a^2 \cdot Cu(d_a) = \frac{\rho_p}{\chi} \cdot d_{ev}^2 \cdot Cu(d_{ev}), \quad (6)$$

where, d_{ev} is the volume equivalent diameter (diameter of a sphere having the same volume as the particle), ρ_p is the density of the particle material, χ is the dynamic shape factor (equal to 1 for spherical particle), Cu is the Cunningham slip correction factor (is value is close to 1 for particle diameters above 3 µm), ρ_0 is the reference density defined for the aerodynamic diameter (ρ_0 = 1000 kg.m^{-3}) and d_a is the aerodynamic diameter.

By using this relation, assuming spherical particles of stainless steel (ρ_p = 8000 kg.m^{-3}), the median diameter equal to 4.7 µm determined by *Morphologi G3* analysis correspond to an aerodynamic value of 13.3 µm. The Figure 14 represents the particle size distribution obtained for aerodynamic diameter from the log normal fit determined on fig 11 together with the different conventional fractions.

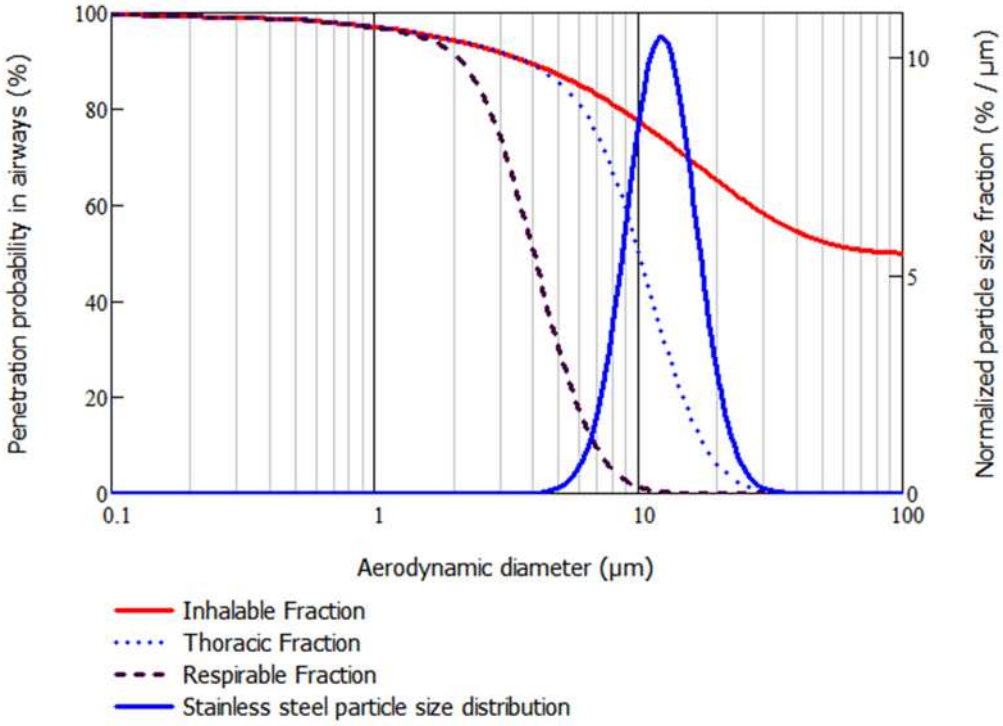

Figure 14: Stainless steel particles size distribution according to aerodynamic diameter, comparison with conventional aerosol size fractions

Result obtained on Figure 14 show that only a few part of the stainless steel particles size distribution is in the range of the respirable fraction. The main part of the particles lies in the inhalable fraction. The precise calculation of each fraction is obtained by convoluting the particle size distribution by each curve defining the conventional fractions. The values obtained are 72 % for the inhalable fraction, 30 % for the thoracic fraction and 1 % for the respirable fraction. These values means that for a concentration of 1 $mg.m^{-3}$ of an aerosol with the considered size distribution (aerodynamic median diameter equal to 13.3 µm and geometric standard deviation of 1.35), the concentration of inhalable particles is only 0.72 $mg.m^{-3}$, the concentration penetrating the thoracic region is 0.3 $mg.m^{-3}$ and the concentration penetrating alveolar region is 0.01 $mg.m^{-3}$.

3.2 Final strategy for steel particle production

Taking into account the weak rate of steel particle production by cutting, the alternative way using surrogate particles is the proposed solution. The size range of the GF powder is in the same range that the particle produced during cutting phase of 316L pipes.

The morphology of the particles from the GF powder is strongly different from the real case (particle produced by cutting). However, the spheroidal geometry is an advantage to control the evolution of the powder in the different step of the process.

Consequently, to produce enough steel powder for the coming *in vitro* and *in vivo* studies, the strategy should use the GF powder. The control characteristics of this powder are interesting for the reproducibility of the coming experiments concerning the tritium loading, the following step in the WP3.

4 Conclusions

This work aimed to develop the method for producing particles in a reproducible manner in terms of composition, morphology and size range for the *in vivo* and *in vitro* studies of TRANSAT WP3.

In order to carry out this work, a facility to produce, collect and analyse steel particles from pipe cutting has been set up. This device has proven to be effective in measuring, during cutting, the distribution of particle diameters in the emitting aerosol. Despite the limited volume of the experiment (about 250 L), the results are in agreement with those reported at the full scale. However, the production rate is about 70 µg/min, which is too low to produce the hundreds of milligrams required within a reasonable time for the TRANSAT project.

However, the description of the particles produced during cutting in 316L by a reciprocating saw, i.e. under realistic conditions, made it possible to define criteria for selecting substitute particles. We were thus able to select the commercial powder GF with a median diameter of 4.7 µm, close to that of the particles produced during 316L cutting with an geometric mean diameter of 4.1 µm. Compared to the conventional aerosol size fraction, the particles from the GF powder are 72 % in the inhalable fraction, 30 % in the thoracic fraction and 1 % in the respirable fraction.

This powder will be used for further studies.

5 References

Paquet, F., Metivier, H. (2009) J. Radiol. Prot. 29(2), 175-181.

Gensdarmes, F. (2003) Effet de la sédimentation sur l'épuration d'un aérosol polydispersé dans une enceinte, application à l'étude de la mise en suspension par chute de poudre. Rapport technique IPSN/DPEA/SERAC/LPMA/03-14.

Bernard, J., Pilot, G. et Grandjean, J.P. (1998) Evaluation of various cutting techniques suitable for the dismantling of nuclear components. Rapport EUR 17919.

Newton, G. J., Hoover, M. D., Barr, E. B., Wong, B. A, Ritter, P. D. (1987) Am. Ind. Hyg. Assoc. J. 48(11), 922-932

Renoux, A., Boulaud, D., Les aérosols. Physique et métrologie, Edition Lavoisier, Technique et Documentation, Paris, (1998).

Baron, P.A., Willeke, K., Aerosol measurement: Principles, techniques and applications (2001).

Vincent, J.H., Aerosol Science for Industrial Hygienists. Pergamon, Elsevier Science Ltd., Oxford. (1995) 238-303.

6 Annexes

Some aggregates of Au/Pd particles are observed on the filter surface. Indeed Au/Pd alloy is used to metallise the sample to avoid charging during SEM observations. The Au/Pd particles are mainly tiny (*i.e.* below 1 µm) and cover uniformly the sample surface. However some aggregates can occur.

Some particles bigger than 50 µm are also observed. They are present regularly on the filter but in small amount. In any case they are not steel particles neither Au/Pd as shown by EDS spectrum and EDS map.

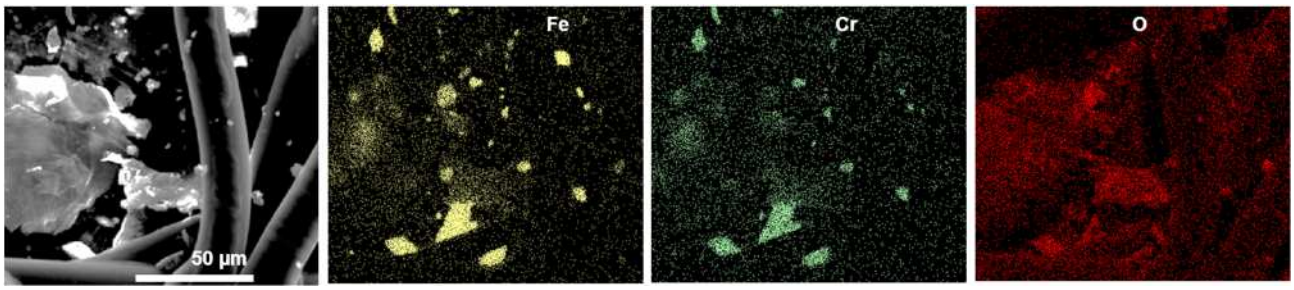

Figure 15: SEM observation using EDS sensor highlighting Fe and Cr (which corresponds to steel particles). Some particle as the biggest one (on the left) is not identified.